

# Einstein-Podolsky-Rosen Paradox in Quantum Diagrams

S.V.Gantsevich

*Ioffe Institute of Russian Academy of Sciences,*

*Saint-Petersburg 194021, e-mail: sergei.elur@mail.ioffe.ru*

*Quantum diagrams are the best language for Quantum Mechanics since they show not only a final result but also the physical process which leads to the result. The quantum correlation at a distance better known as the Einstein-Podolsky-Rosen paradox may be easily understood being depicted in the time-ordered quantum diagrams. In the diagrams one can clearly see what the so-called entangled quantum states really are and how they contribute to the violation of Bell inequality. The wave function phase relations that are the actual physical "common cause in the past" for the observed correlation become also visual and evident. Thus the diagram analysis shows that the phenomenon of distant quantum correlation has simple causal and local explanation and there is no need to invent various extravagant constructions contradicting the established physical principles as well as usual common sense considerations.*

Pacs: 71.10.Ca, 72.70.+m, 05.30.-d, 05.40.-a

## I. INTRODUCTION

In recent decades it was found experimentally that physical quantities separated by space-like intervals can be correlated. Logically the correlation between two events in one time moment is possible either by their mutual interaction or by some "common cause in the past". However, Relativity Theory forbids the infinite interaction velocities whereas Quantum Mechanics states that the values of measured physical quantities do not exist before the measurements.

Thus it seems that both reasons for the observed correlation should be excluded if one equally accepts RT and QM. The apparent contradiction between them was formulated in 1935 by Einstein, Podolsky and Rosen [1] being named subsequently the EPR-paradox. After the immediate Bohr reply [2] defending the QM consistency the paradox was forgotten for years. In 1951 Bohm proposed its very convenient spin-version [3] and then in 1964 Bell constructed his famous inequality [4] that made possible the experimental verification of EPR(B) quantum correlation.

The violation of the Bell inequality in the EPR(B) experiments [5-8] proved the validity of QM predictions and made actual the adequate interpretation of the quantum correlation at large distances.

These experiments triggered the enormous incessant flow of literature with various explanations of the paradox and interpretations of quantum mechanics (see, e.g. [9-17]).

In order to overcome the explanation difficulty one frequently resorts to various strangely-looking constructions like "momentary action at a distance", "retrocausality", "multitude of worlds" etc. All such inventions contradict the traditional physical picture going from the time of Faraday and Maxwell as well as the usual common sense.

Recently the very ingenious experiments [18] confirming once more with high reliability the violation of Bell inequality was proclaimed as the final proof of the so-called nonlocality of QM and the total crash of the point-to-point Faraday-Maxwell interaction picture that allegedly followed from QM [19].

Actually the observed correlation is the macroscopic version of the quantum exchange correlation well-known in the microscopic quantum systems like atoms, molecules or gases.

However, because of its microscopic character this phenomenon attracted little attention and the words "it was a quantum effect" usually was enough for an explanation.

In order to see better the nature and origin of various quantum effects it is convenient and instructive to represent them in quantum-mechanical diagrams. The diagrams are the best language for QM and in some sense their role may be compared with the role of Leibnitz-Newton Calculus for Classical Mechanics. One may say without much exaggeration that to study QM without diagrams is the same as to study Classical Physics not using the differentiation and integration.

However, the graphics of widely used Feynman diagrams is not fit for correlation phenomena. The Feynman pictures have no time ordering of event-points and do not explicitly show the occupancy numbers of quantum states. All this is highly important for the understanding of the physics of correlation. Therefore, we shall use below the kinetic diagrams which we used in the past for various kinetic problems (see, e.g.([<sup>20,21</sup>])). What follows below may be regarded as the graphic illustration of the analytical formulae of the paper [<sup>22</sup>] about exchange correlation phenomena.

## II. DIAGRAMS

The kinetic diagrams have one-to-one correspondence with the analytical formulae and can be easily and rather unambiguously interpreted. We shall not introduce them here in a formal way. Instead we shall show how to depict them using Feynman diagrams as prototypes. Since the diagram topology and the meaning of points and lines are the same in both types of diagrams this can be done without efforts.

A diagram is the collection of lines with points on them. The lines correspond to probability amplitudes (or simply to wave functions). Generally they are the eigenfunctions of the basic Hamiltonian and are marked by the corresponding indices. The points relate to the actions of perturbation potentials or to the observable quantities. The points are proportional to the matrix elements of corresponding operators. The event-points in kinetic diagrams have strict time order and in addition to the lines there are special symbols for the occupancy numbers of quantum states.

Unlike them the Feynman diagrams have no time order for points and their lines do not distinguish between wave functions and the wave functions with the occupancy numbers. Because of this a single Feynman diagram generally describes a number of various physical processes and in order to treat them adequately some additional analytical procedures are required. The necessity of additional analytic calculations as well as the polysemy of Feynman diagrams hamper their use for the interpretation of correlation phenomena.

To the contrary one kinetic diagrams corresponds as a rule to one concrete physical process and one final analytical expression. Hence many kinetic diagrams correspond to one Feynman diagram. The large number of kinetic diagrams is the price for the simplicity of rules and the unambiguity of interpretation.

As a simple example let us take the expression for the mean value of an observable physical quantity, represented by the operator  $A$ , in a quantum state  $u$  occupied with the probability  $F_u$ .

$$\bar{A} = \langle u|A|u\rangle F_u \quad (1)$$

Here  $|u\rangle \equiv \psi$  is the wave function of the state  $u$  or  $u$ -ket and  $\langle u| \equiv \psi^\dagger$  is its complex conjugation or  $u$ -bra. Note that the bra and ket functions that are necessary to obtain a physical observable are *different quantities with their own time and space dependences*. The quantity  $F_u$  is the occupancy number of the state  $u$  or its distribution function. The values of  $F$  lie in the range  $[0, 1]$  for one observable particle and can be arbitrary for a coarse grained averaged ensemble of many particles.

Now let us depict this formula as the Feynman and kinetic diagrams (see Fig.1). The diagrams have only one point so there is no need for the time ordering (in the picture time goes upwards). Looking on the Feynman diagram at the left we see that it does not fully

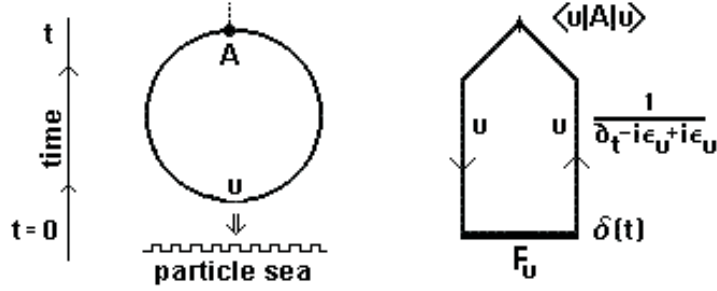


FIG. 1: Observed quantity  $A$  in quantum state  $u$

correspond to the expression (1).

At first the occupancy number  $F_u$  is absent. Then we see only one line for the  $u$ -bra and  $u$ -ket functions in (1).

The kinetic diagram at the right has one-to-one correspondence with the formula (1). Reading it from top to bottom (i.e. against the time) and writing one by one all symbols we have:

$$\langle u|A|u \rangle \frac{1}{\partial_t - i\epsilon_u + i\epsilon_u} \delta(t) F_u = \langle u|A|u \rangle \frac{1}{\partial_t} \delta(t) F_u = \langle u|A|u \rangle F_u \Theta(t) \quad (2)$$

Here  $\Theta(t) = (1/\partial_t)\delta(t)$  is the Heaviside step function equal to zero at  $t < 0$  and unity at  $t \geq 0$ . We see that in addition to (1) the diagram shows the time dependence of the bra and ket functions.

The resolvent  $1/(\partial_t - i\epsilon' + i\epsilon)$  which corresponds to the bra+ket line section between the observation point at  $t$  and the initial point at  $t = 0$  is the solution of the double Schrödinger equation governing the combine evolution of the bra and ket functions.

$$\frac{1}{\partial_t - iH' + iH} \overline{\psi^\dagger(0)\psi(0)} \delta(t) = e^{i(H' - H)t} \overline{\psi^\dagger(0)\psi(0)} \Theta(t) \quad (3)$$

For the eigenfunctions of the Hamiltonian the resolvent contains only its eigenvalues  $\epsilon$  and  $\epsilon'$ . The energies (frequencies) of ket-lines enter in the energy denominator with the plus sign and those of bra-lines with the minus sign. In the Feynman-type diagram techniques the external frequency  $\omega$  or the Laplace parameter  $s$  appear in the resolvent instead of the time derivative  $\partial_t$ . The use of  $\partial_t$  is preferable since it combines visual time pictures with the simplicity of Laplace or Fourier formulae. We can attribute the symbol  $\partial_t$  to the time line and then add it to the bra and ket energies in the energy denominator. (Note that the diagrams always represent not time equations but their solutions).

In order to form the occupancy number  $F_u$  at  $t = 0$  the initial phases of bra and ket should be equal and opposite in signs. The phase equality survives during time evolution so that the phases cancel each other and do not appear explicitly in (1).

The topology as well as the time or frequency dependence in both types of diagrams are always the same. Apart from the time ordering of points the main difference is the presence of the occupation numbers  $F$  in the kinetic diagrams. If in kinetic diagrams we include these symbols into lines we will get the corresponding Feynman diagrams.

The transition from a Feynman diagram to the set of corresponding kinetic diagrams is also simple but requires some practice for diagrams with many points and lines. After the time ordering of points the occupation numbers can be introduced by the following graphic procedure:

Let us imagine that we have a "sea of particles" below  $t = 0$  in the diagram (see Fig.1). If we take a line of the diagram and then plunge it into this sea the line will emerge with the tail-symbol representing the occupancy number. The tail divides the initial line into

the bra-line and ket-line with the same quantum index and *the same value of initial phase*. In any kinetic diagram at least one of the lines should have this tail. This simple graphic procedure may substitute the complicated analytical correspondence rules which apply to Feynman diagrams when one uses them for cases where the occupancy numbers are not equal to zero or unity.

The physical sense of the kinetic diagram in Fig.1 is simple and transparent. With the probability  $F_u$  we have the quantum state  $u$  at  $t = 0$  formed by the product of u-bra and u-ket. It is important that their initial (arbitrary) phases coincide and therefore cancel each other:  $e^{+i\varphi_u}e^{-i\varphi_u} = 1$ . If u-bra and u-ket have different arbitrary phases their product will vanish after phase averaging and there will be no permanent occupation of the quantum state  $u$ . The occupation number  $F_u$  may be regarded as a number of u-bra and u-ket with the coinciding phases at  $t = 0$ . During time evolution the u-bra and u-ket acquire (under permanent action of the Hamiltonian) the same phases  $e^{+i\epsilon_u t}e^{-i\epsilon_u t} = 1$ . (The convolution of these functions appears as the resolvent in Fig.1). Then the occupancy number of state  $u$  remains unchanged  $F_u(t) = F_u(0)$  as well as the expectation value of the physical quantity  $A$  in this state.

### III. EXCHANGE CORRELATION

Now let us consider two independent quantum states  $u$  and  $v$  occupied with the probabilities  $F_u$  and  $F_v$  and two observable physical quantities  $A$  and  $B$ . We suppose that these two quantities are measured by two independent detectors. We suppose also that we make the series of measurements and can compare their results made in the same time moment  $t$ .

Now let us depict the matrix element  $\langle uv|AB|uv\rangle F_u F_v$  which we identify with the jointly averaged product of the measurement values in both detectors. Two kinetic diagrams for this quantity are presented in the Fig.2. Two analogous diagrams can be obtained by the substitution  $u \leftrightarrow v$ . For brevity we do not draw them. We see in the picture the sum

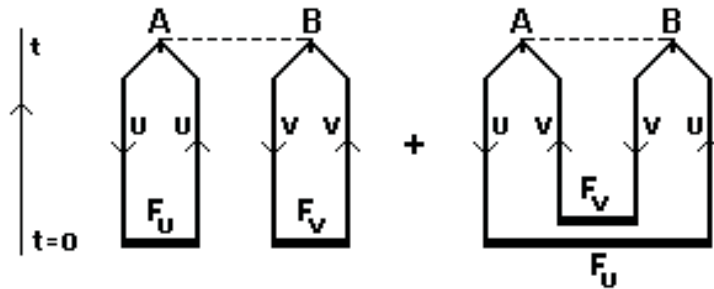


FIG. 2: Exchange correlation for two measurements

of two diagrams with different topology. The left diagram consists of two objects with no links between them (the apical correlation line should not be counted). The states  $u$  and  $v$  are represented by the bra and ket lines with the same indices which form at  $t = 0$  two independent occupancy numbers. So we have two pure (bra+ket) pairs. Then one pair hits one detector while other pair hits another detector.

Reading the diagram we get the product of the independent contributions of two states:

$$\langle u|A|u\rangle\langle v|B|v\rangle\frac{1}{\partial_t - i\epsilon_u + i\epsilon_u - i\epsilon_v + i\epsilon_v}\delta(t)F_uF_v = \langle u|A|u\rangle\langle v|B|v\rangle F_uF_v\Theta(t)$$

The analogous result  $\langle v|A|v\rangle\langle u|B|u\rangle F_uF_v$  comes from the omitted diagram with  $u \leftrightarrow v$ . This way we get the uncorrelated contribution to  $\overline{AB}$  as the sum:

$$(\overline{AB})_{uncor} = [\langle u|A|u\rangle\langle v|B|v\rangle + \langle v|A|v\rangle\langle u|B|u\rangle]F_uF_v. \quad (4)$$

The diagrams have strict correspondence to the QM rules being their visualization. We have two measurements and it seems that these measurements relate also to two objects namely to two observed quantum particles. Indeed we have two states and two occupation numbers. But the diagrams clearly show that there are *four entities* represented by *four lines*. Each observed quantum particle is represented by the *pair of bra+ket*.

Now let us look at the right diagram of the Fig.2. Its topology demonstrates quite clearly the correlation between  $A$  and  $B$  measurements. Here we see also two bra+ket pairs at  $t = 0$  and two bra+ket pairs entering the detectors. But unlike the left diagram now the detector pairs and the occupancy number pairs are different. The initial  $(u, u)$  and  $(v, v)$  pairs become  $(u, v)$  and  $(v, u)$  pairs of the detector devices. The bra and ket have their own time and space coordinates and just this fact makes the exchange possible. (In the same way a quantum particle (i.e. bra+ket pair) can travel through both slits in the two-slit interference being therefore in one time moment in two different space points.)

Reading the diagrams from top to bottom and writing consecutively all symbols we get

$$\langle u|A|v\rangle\langle v|B|u\rangle\frac{1}{\partial_t - i\epsilon_u - i\epsilon_v + i\epsilon_v + i\epsilon_u}\delta(t)F_uF_v = \langle u|A|v\rangle\langle v|B|u\rangle F_uF_v\Theta(t) \quad (5)$$

The omitted analogous diagram gives the expression with  $u \leftrightarrow v$  so the correlated  $\overline{AB}$  contribution is given by

$$(\overline{AB})_{cor} = \pm[\langle u|A|v\rangle\langle v|B|u\rangle + \langle v|A|u\rangle\langle u|B|v\rangle]F_uF_v \quad (6)$$

The total average  $\overline{AB}$  is the sum of the uncorrelated and correlated parts:

$$\overline{AB} = [\langle u|A|u\rangle\langle v|B|v\rangle \pm \langle u|A|v\rangle\langle v|B|u\rangle]F_uF_v + (u \rightleftharpoons v). \quad (7)$$

The sign of correlation contributions is positive for bosons and negative for fermions. For fermions the correlation contribution diminishes the uncorrelated value e.g.  $\overline{AB} \equiv 0$  in the limit  $u = v$ . For bosons the situation is inverse and the correlation increases the uncorrelated value.

The right diagram in the Fig.2 without F-symbols becomes the well-known Feynman loop-diagram. The loop can be redrawn as the kinetic correlation diagram by the line plunging procedure described above in the Fig.1. Also the right connected diagram of the Fig.2 can be obtain from the left unconnected diagram by the line exchange. Graphically the exchange of lines inevitably leads to the their intersection or, one may say, to their "*Verschränkung*" alias "*entanglement*". (For better transparency the correlation diagram in Fig.2 is depicted in a more compact form without line intersection.)

The diagrams and the corresponding formulae demonstrate the existence of the correlation between non-interacting quantum particles which reveals itself as the correlation of observable physical quantities. One should emphasize that the correlation emerges only after the joint averaging of detector data. The data averaged separately in both detectors give simply the sum of independent contributions of both states:

$$\begin{aligned} \overline{A} &= \langle u|A|u\rangle F_u + \langle v|A|v\rangle F_v \\ \overline{B} &= \langle u|B|u\rangle F_u + \langle v|B|v\rangle F_v \end{aligned} \quad (8)$$

These expressions have no trace of correlation and correspond to the uncorrelated part  $(\overline{AB})_{uncor}$  in (4).

Now let us discuss the physical reason for the absence of the exchange contribution in (8) and its presence in (7).

These different results follow from the same series of concrete measurements in both detectors and differ only by the averaging procedures. Therefore the exchange contribution should be *always present* in the concrete measurement data in both detectors. It vanishes after separate averaging and emerge after joint averaging of detector data.

We can see how and why it occurs in the diagrams for the separate measurements in two detectors (see Fig.3). The sum of diagrams at the left describes the contributions of  $(u, u)$  and  $(u, v)$  bra-ket pairs entering the detector  $A$  while the diagram sum at the right corresponds to the analogous contributions of  $(v, u)$  and  $(v, v)$  pairs into the detector  $B$ . (The diagrams with  $u \leftrightarrow v$  are analogous and for brevity we do not depict them).

The left and the right parts of the diagram sums (together with analogous  $u \leftrightarrow v$  diagrams) give the formulae (8). These expressions do not depend on phases and time and give always the same result either for separate or for joint averaging of concrete detector data.

The diagram in the middle of the Fig.3 is the dissected correlation diagram of the Fig.2. It describes the contributions of the mixed  $(u, v)$  and  $(v, u)$  bra-ket pairs. The disrupted F-symbols show that their bra and ket import into detectors separately their initial amplitudes and phases. They belong to different occupied states and therefore their separate contributions to the detectors are time and phase dependent.

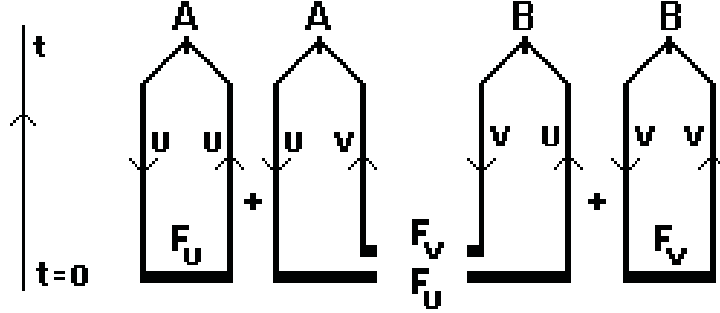


FIG. 3: Measurements in separate detectors

Reading the middle diagram related to the detector  $A$  we get:

$$\langle u|A|v\rangle \frac{1}{\partial_t - i\epsilon_u + i\epsilon_v} \delta(t) \sqrt{F_u F_v} e^{i\varphi_u} e^{-i\varphi_v} = \langle u|A|v\rangle e^{i(\epsilon_u - \epsilon_v)t + i(\varphi_u - \varphi_v)} \sqrt{F_u F_v} \Theta(t) \quad (9)$$

Here  $\sqrt{F_u}$  and  $\sqrt{F_v}$  are the amplitudes of bra and ket while  $\varphi_u$  and  $\varphi_v$  are their initial phases.

The other part of this diagram gives the analogous expression for the detector  $B$ :

$$\langle v|B|u\rangle \frac{1}{\partial_t - i\epsilon_v + i\epsilon_u} \delta(t) \sqrt{F_u F_v} e^{i\varphi_v} e^{-i\varphi_u} = \langle v|B|u\rangle e^{i(\epsilon_v - \epsilon_u)t + i(\varphi_v - \varphi_u)} \sqrt{F_u F_v} \Theta(t) \quad (10)$$

The expressions (9) and (10) contain the oscillating phase multipliers  $e^{i\phi(t)}$  and  $e^{-i\phi(t)}$  which become zero after averaging over the initial phases or over time (for  $\epsilon_u \neq \epsilon_v$ ). Thus, despite the presence of the mixed bra-ket pairs in the detectors their contributions do not appear in the detector data averaged separately. The expressions (8) describe just the result of such averaging.

Quite contrary in the expression (7) for  $\overline{AB}$  (depicted in Fig.2) the  $(u, v)$  and  $(v, u)$  mixed pairs contributions appear as the product with  $e^{i\phi(t)} e^{-i\phi(t)} = 1$  and survive under joint averaging of the detector data.

Thus just this exchange contribution which cannot be observed in separate detectors is the physical cause of correlation of two detectors. Let us emphasize that this *common cause in the past* is the real reason for the correlation and not the mythical "momentary spooky action at a distance" with the mysterious "mutual influence of measurements". The correlation takes place for any physical quantities  $A$  and  $B$ .

Two mixed bra+ket pairs of the dissected diagram in Fig.3 are just the mysterious "entangled quantum particles". They have the same (and sign-opposite) values of initial phase

difference and conserve them during the time evolution. The mutual phase coherence of such mixed (bra+ket) pairs can hold at very large time and space intervals in the absence of perturbations. Just the presence of such mutually correlated mixed (bra+ket) pairs ensures the quantum exchange correlation observed at large macroscopic distances.

#### IV. EPR(B) SPIN CORRELATION

For the EPR(B) spin correlation the operators  $A$  and  $B$  are the scalar products of the spin vector  $\sigma$  formed by the Pauli matrices and the arbitrary unit vectors  $a$  and  $b$ . The ket functions  $|u\rangle \equiv |\uparrow\rangle$  and  $|v\rangle \equiv |\downarrow\rangle$  now are the eigenfunctions of  $\sigma_z$  with the eigenvalues  $s_\uparrow = 1$  and  $s_\downarrow = -1$ . In polar coordinates the spin operator  $S$  is given by

$$S \equiv (\mathbf{n}, \sigma) = \sin \theta \cos \varphi \sigma_x + \sin \theta \sin \varphi \sigma_y + \cos \theta \sigma_z$$

and its diagonal matrix elements are

$$\langle \uparrow | S | \uparrow \rangle = \cos \theta \langle \uparrow | \sigma_z | \uparrow \rangle = \cos \theta, \quad \langle \downarrow | S | \downarrow \rangle = \cos \theta \langle \downarrow | \sigma_z | \downarrow \rangle = -\cos \theta. \quad (11)$$

while the nondiagonal elements is given by

$$\begin{aligned} \langle \uparrow | S | \downarrow \rangle &= \cos \varphi \sin \theta \langle \uparrow | \sigma_x | \downarrow \rangle + \sin \varphi \sin \theta \langle \uparrow | \sigma_y | \downarrow \rangle = e^{i\varphi} \sin \theta, \\ \langle \downarrow | S | \uparrow \rangle &= \cos \varphi \sin \theta \langle \downarrow | \sigma_x | \uparrow \rangle + \sin \varphi \sin \theta \langle \downarrow | \sigma_y | \uparrow \rangle = e^{-i\varphi} \sin \theta. \end{aligned} \quad (12)$$

Using (11) and (12) we get from (7) the correlation of spins measured in the directions  $\mathbf{n} = \mathbf{a}$  and  $\mathbf{n} = \mathbf{b}$ :

$$\overline{AB} = -\cos \gamma 2F_\uparrow F_\downarrow \quad (13)$$

Here  $\gamma$  is the angle between the measured spin directions

$$\cos \gamma = \cos \theta_a \cos \theta_b + \cos(\varphi_a - \varphi_b) \sin \theta_a \sin \theta_b$$

The first item here comes from the diagram without correlation in Fig.2 (i.e. from the expressions (4) while the second item comes from the exchange diagram (i.e. from the expressions (6)). The sum of them (7) becomes independent of the direction of the spin vector  $\sigma$  being proportional to the scalar product of the unit vectors  $\mathbf{a}$  and  $\mathbf{b}$ .

Usually one gets the expression for  $\overline{AB}$  as a matrix element  $\langle \Psi | AB | \Psi \rangle$  where  $\Psi$  is the two-particle singlet wave function

$$\Psi = (|\uparrow_a\rangle |\downarrow_b\rangle - |\uparrow_b\rangle |\downarrow_a\rangle) / \sqrt{2} \quad (14)$$

Using  $\Psi$  we get

$$\overline{AB} = \langle \Psi | AB | \Psi \rangle = -\cos \gamma \quad (15)$$

and

$$\overline{A} = \langle \Psi | A | \Psi \rangle = 0, \quad \overline{B} = \langle \Psi | B | \Psi \rangle = 0 \quad (16)$$

These expressions are equal to the previous expressions under conditions  $F_\uparrow = F_\downarrow$  and  $F_\uparrow F_\downarrow = 1/2$ .

One frequently treats the identity  $\langle \Psi | S | \Psi \rangle = 0$  for any spin direction as some peculiar property of the singlet function (14) which is "maximally entangled". The expressions (16) correspond to the expressions (8) for the mean detector data from two independent sources. These expressions for two spins take the form:

$$\begin{aligned} \overline{A} &= \langle \uparrow | A | \uparrow \rangle F_\uparrow + \langle \downarrow | A | \downarrow \rangle F_\downarrow = \cos \theta_a (F_\uparrow - F_\downarrow), \\ \overline{B} &= \langle \uparrow | B | \uparrow \rangle F_\uparrow + \langle \downarrow | B | \downarrow \rangle F_\downarrow = \cos \theta_b (F_\uparrow - F_\downarrow). \end{aligned} \quad (17)$$

For equal number of opposite spins  $F_{\uparrow} = F_{\downarrow}$  we have  $\bar{A} = \bar{B} = 0$ .

One should also remember that the correlation is of statistical nature and to observe it a series of measurements is required. The Malus law for a flow of polarized spins measured at some angle is realized as random series of positive and negative units that appear with the probabilities of positive and negative results:

$$\cos \theta = (+1) \cos^2 \theta/2 + (-1) \sin^2 \theta/2 = \cos^2 \theta/2 - \sin^2 \theta/2. \quad (18)$$

As we see from (17) for two spin flows of the opposite signs the mean observed value is proportional to the difference of intensities of the flows:

$$\bar{S} = \langle \uparrow |S| \uparrow \rangle F_{\uparrow} + \langle \downarrow |S| \downarrow \rangle F_{\downarrow} = \cos \theta (F_{\uparrow} - F_{\downarrow}). \quad (19)$$

The observation of spins in the singlet states gives zero mean value for any measurement direction just because of the parity of intensities  $F_{\uparrow} = F_{\downarrow}$ . This parity is the unique real property of the singlet state. For  $\theta = \pi/2$  the detector always gives mean zero irrespective of the flow intensity. In this case there will be equal average number of positive and negative units fixed by the detector.

Now let us see how the Bell inequality is violated by the quantum exchange correlation. We choose two directions  $\mathbf{a}$  and  $\mathbf{a}'$  of the detector  $A$  and two directions  $\mathbf{b}$  and  $\mathbf{b}'$  of the detector  $B$ . Suppose that all vectors lay in the plane  $(z, x)$ . The vectors  $\mathbf{a}$  and  $\mathbf{b}$  are parallel and  $\theta_a = \theta_b = 0$ . The vectors  $\mathbf{a}'$  and  $\mathbf{b}'$  are mutually orthogonal and  $\theta_{a'} = -\theta_{b'} = \pi/4$ . The Bell sum of  $AB$  spin data correlation where the spin values  $A$  and  $B$  are always equal to  $\pm 1$  is given by

$$|A(B + B') + A'(B - B')| = |AB + AB' + A'B - A'B'| = |1 + 1 + 1 - 1| = 2$$

Taking  $AB$ -products as  $\cos \gamma$  we have for chosen detector directions the corresponding QM expression:

$$|\cos \gamma_{ab} + \cos \gamma_{ab'} + \cos \gamma_{a'b} - \cos \gamma_{a'b'}| = |1 + 1/\sqrt{2} + 1/\sqrt{2} - 0| = 1 + \sqrt{2} > 2$$

Note that in this expression the values of first three terms come only from the uncorrelated part of  $\cos \gamma$  in (13) because of  $\sin \theta_a = \sin \theta_b = 0$  and the correlated part is absent. The value of fourth term  $A'B' \rightarrow \cos \gamma_{a'b'} = \cos(\pi/2) = 0$  is the sum of the both parts of (13) which cancel each other. If we exclude the correlated contribution the sum will satisfy the Bell inequality:  $|1 + 1/\sqrt{2} + 1/\sqrt{2} - 1/2| = 1/2 + \sqrt{2} < 2$ . We see that the Bell inequality is violated just because of the presence of the mutually correlated contributions in both detectors.

## V. COULOMB EXCHANGE INTERACTION

In the EPR(B) correlation experiments the enormous efforts were made to exclude any real or imaginal link between detectors. At last all rivals of the instantaneous (spooky) action at a distance were removed [18] and the incontestable nonlocality of QM (and all nature) was solemnly proclaimed [19].

Since the observed correlation has no relation to this mythical phenomenon and can be simply explained by the common cause in the past, it seems that the "struggle with loopholes" is a little redundant. The real problem in correlation experiments is to compare just those detector data that relate to mutually correlated fluctuations over the permanent uncorrelated background. For this purpose one can use some real fast interaction between the mutually correlated events.

Let us consider one such case where two observation points are connected by real (quasi)momentary interaction. This case is the Coulomb interaction of charged particles

in a quantum system. The fast Coulomb interaction may connect randomly appearing charges and serve as the indicator of correlation. The effect can be depicted in diagrams.

Above we treated the horizontal apical lines in Fig.2 as the comparison signals for the detector data fixed in the same time  $t$  in both detectors.

Now let these lines represent the Coulomb potential  $1/(|\mathbf{r} - \mathbf{r}'|)$  between charges at the points  $\mathbf{r}$  and  $\mathbf{r}'$ . The appearing charges play a role of detecting devices in these points for the electron states  $u$  and  $v$ . For better agreement with usual formulae we take the case  $F_u = F_v = 1$ . Reading the diagrams we get the well-known expression for the Coulomb interaction energy of two electrons ( $e$  is the electron charge):

$$W = e^2 \int_V d\mathbf{r}d\mathbf{r}' \left[ \frac{|\psi_u(\mathbf{r})|^2 |\psi_v(\mathbf{r}')|^2}{|\mathbf{r} - \mathbf{r}'|} - \frac{\psi_u^\dagger(\mathbf{r}) \psi_v(\mathbf{r}) \psi_v^\dagger(\mathbf{r}') \psi_u(\mathbf{r}')}{|\mathbf{r} - \mathbf{r}'|} \right] \quad (20)$$

The first term corresponds to the left (uncorrelated) diagram in Fig.2 whereas the second term corresponds to the right (correlated) diagram. (The contributions of the omitted diagrams with  $(u \leftrightarrow v)$  in Fig.2 are included automatically in (20) because of the double integration over space).

The uncorrelated first term in (20) has the simple and clear meaning. Two charge clouds with the densities  $e|\psi_u(\mathbf{r})|^2$  and  $e|\psi_v(\mathbf{r}')|^2$  interact by the Coulomb potential. The clouds are formed by pure bra+ket pairs and do not depend on their phases and time. This contribution to the energy does not differ from analogous classical expressions.

The second term in (20) is usually called the exchange energy and according to QM manuals and books its existence is a quantum effect which has no classical analogy. Let us note by the way that the Planck constant  $\hbar$  being explicitly written does not appear in this expression. Also the Coulomb potential definitely points out that it is the interaction of electric charges. But what charges? Are they different from the charges in the first term? And why?

Let us substitute one integration variable in the Coulomb potential in (20) by an external variable  $\mathbf{R}$ . The substitution kills the exchange energy term since  $\langle u|v \rangle = \langle v|u \rangle = 0$  (also  $\langle u|u \rangle = \langle v|v \rangle = 1$ ). Then we come to the expression for the energy of electrostatic field measured by the test charge  $e$  at the point  $\mathbf{R}$ :

$$W(\mathbf{R}) = e^2 \int_V d\mathbf{r} \frac{|\psi_u(\mathbf{r})|^2}{|\mathbf{r} - \mathbf{R}|} \quad \text{or} \quad W(\mathbf{R}) = e^2 \int_V d\mathbf{r}' \frac{|\psi_v(\mathbf{r}')|^2}{|\mathbf{R} - \mathbf{r}'|} \quad (21)$$

Here one electron is used as a test charge. An external unit test charge would show the electrostatic fields  $\Phi(R)$  created by two independent charge distributions:

$$\Phi(R) = e \int_V d\mathbf{r} \frac{|\psi_u(\mathbf{r})|^2}{|\mathbf{R} - \mathbf{r}|} + e \int_V d\mathbf{r}' \frac{|\psi_v(\mathbf{r}')|^2}{|\mathbf{R} - \mathbf{r}'|} \quad (22)$$

The interaction of two charge distributions (22) leads to the first part of the expression (20) which corresponds to the uncorrelated diagram in Fig.2. The diagram shows that the charges at points  $\mathbf{r}'$  and  $\mathbf{r}$  are produced by the pure bra+ket pairs and therefore do not depend on their phases.

Quite contrary in the exchange energy expression in (20) the mixed  $(uv)$  and  $(vu)$  bra+ket pairs appear together at the points  $\mathbf{r}'$  and  $\mathbf{r}$ . A mixed pair has random phase and therefore the charge it produces at a given point is the charge fluctuation with mean zero values. Averaged separately over the initial phase difference or observation time these charge fluctuations vanish in each point. But the  $(uv)$  and  $(vu)$  charge fluctuations are mutually correlated so that while appearing they have time to interact and give non-zero contributions to the mean interaction energy. The equal phase values of these mixed bra+ket pairs cancel each other and do not enter explicitly in the final expression (20). The presence of correlated random charge fluctuations may be illustrated by the diagrams in Fig.3.

## VI. CONCLUSION

The electron exchange correlation as well as many other microscopic quantum correlation effects have the same physical nature as the macroscopic EPR-correlation. The resemblance between this correlation and various microscopic correlation phenomena was marked from time to time in the literature but usually as the universal manifestation of nonlocality and instantaneous links between quantum states.

On the one hand, it is highly doubtful that the application of such non-physical phantasies can improve the understanding of microscopic correlation mechanisms. On the other hand, the abstruse EPR-paradox in reality has simple physical explanation and just this explanation can help to clarify much more utilitarian effects.

- 
- <sup>1</sup> A.Einstein, B.Podolsky, N.Rosen, Phys. Rev., **47**, 777 (1935).  
<sup>2</sup> N.Bohr, Phys. Rev., **48**, 696 (1935).  
<sup>3</sup> D.Bohm and Y.Aharonov, Phys. Rev. **108**, 1070 (1957).  
<sup>4</sup> J.S.Bell, Physics 1, 195, (1964)  
<sup>5</sup> A.Aspect, J.Dalibard, G.Rodger, Phys. Rev. Lett. , **49**, 91 (1982).  
<sup>6</sup> A. Aspect, J.Dalibard, G.Rodger, Phys. Rev. Lett. , **49**, 1804 (1982).  
<sup>7</sup> G.Weih's et al., Phys. Rev. Lett. 81, 5039 (1998)  
<sup>8</sup> N.A.Rowe et al., Nature 409, 791, (2001)  
<sup>9</sup> N.Brunner, D.Cavalcanti, S.Pironio, V.Scarani, S.Wehner, Rev. Mod. Phys. , **86**, 419 (2014).  
<sup>10</sup> M.Navascues and D.Peres-Garcia, Phys. Rev. Lett. , **109**, 160405 (2012).  
<sup>11</sup> S.P.Walborn, A.Salles, R.M.Gomes et al., Phys. Rev. Lett. , **106**, 130402 (2011).  
<sup>12</sup> T.Maudlin, Am.J.Phys, **78**, 121 (2010).  
<sup>13</sup> M.D.Reid, P.D.Drummond, W.P.Bowen et al., Rev. Mod. Phys. , **81**, 1727 (2009).  
<sup>14</sup> L.Amico, R.Fazio, A.Osterloh, V.Vedral, Rev. Mod. Phys. , **80**, 518 (2008).  
<sup>15</sup> J.M.Raimond, M.Brune, S.Haroche, Rev. Mod. Phys. , **73**, 565 (2001).  
<sup>16</sup> W.H.Zurek, Rev. Mod. Phys. , **75**, 715 (2003).  
<sup>17</sup> A.Zeilinger, Rev. Mod. Phys. , **71**, S288 (1999).  
<sup>18</sup> B.Hensen et al., Nature, **526**, 682 (2015).  
<sup>19</sup> H.Wiseman, Nature, **526**, 649 (2015).  
<sup>20</sup> S.V.Gantsevich, V.L.Gurevich, M.I.Muradov et al., Phys.Rev.B, 52, 14006, (1995).  
<sup>21</sup> R.Katilius et al., Fluct.Noise Lett.,**9**,N4, 373, (2010);**12**,N4, 1350023 (2013)  
<sup>22</sup> S.V.Gantsevich, V.L.Gurevich, arXiv:quant-ph/1512.03762 (2016).